Int J Mech Mater Des
https://doi.org/10.1007/s10999-024-09709-5

Material extrusion additive manufacturing of novel lightweight collinear stayed polymer lattices

Yating Ou · Anton Köllner · Antonia Gwendolyn Dönitz · Tim Erik Richter · Christina Völlmecke

Received: 8 December 2023 / Accepted: 22 January 2024

Abstract A novel type of lightweight and high-performance, collinear polymer lattices is presented in which the concept of stayed slender columns is exploited with the aid of material extrusion additive manufacturing (MEX). The stays, preventing lower order buckling, are additively manufactured using the printing strategy bridging. Through conducting experimental test series on representative elements and two-dimensional lattices, it is demonstrated that the 3D printed stayed column lattices exhibit significantly improved compressive strength in comparison with conventional collinear lattices. The potential of introducing deliberate geometric imperfections to affect the structural behaviour is furthermore outlined in the current work.

Keywords Material extrusion additive manufacturing · Metamaterials · Lattices · Lightweight structures · Stayed columns · Buckling

Abbreviations

AM	Additive manufacturing
MEX	Material extrusion additive manufacturing
FDM	Fused deposition modelling
FFF	Fused filament fabrication
STL	Stereolithography
SLM	Selective laser melting
PLA	Polylactic acid

Y. Ou · A. Köllner · A. G. Dönitz · T. E. Richter · C. Völlmecke (✉)
Stability and Failure of Functionally Optimized Structures Group, Institute of Mechanics, Technische Universität Berlin, Einsteinufer 5, 10587 Berlin, Germany
e-mail: christina.voellmecke@tu-berlin.de

1 Introduction

Lightweight structures being characterized by high strength to weight ratios can be found in various applications comprising the aeronautical, automotive and civil engineering sector (Braga et al. 2014; Njuguna 2016; Czerwinski 2021; Acanfora et al. 2023). Due to their slenderness such structures are vulnerable to buckling instabilities that generally govern their design. A common type of lightweight structures, being often used as core material in sandwich constructions, are lattice structures which may be understood as two- or three-dimensional open-celled structures.

With additive manufacturing becoming readily available in recent years, the design and the fabrication of lattice structures made from polymers and metals has been the subject of enormous research activities (e.g. see Askari et al. 2020; Tang et al. 2020; Nazir et al. 2023). Besides the feasibility of the manufacturing of specific lattice structures with various AM techniques (e.g. fused filament fabrication (FFF)/material extrusion additive manufacturing (MEX) (Tang et al. 2020), stereolithography (STL), selective laser melting (SLM) (Maconachie et al. 2019), etc.), optimizing the lattice configuration for

Published online: 30 March 2024

certain load cases or to achieve optimal stiffness/strength properties has been a main driver within the research community (Gorguluarslan et al. 2017; Wang et al. 2020; Li et al. 2023). Collinear lattice structures, being one of the most simple configurations, still represents a common choice as core material in sandwich panels. As most lattice structures, but being particularly relevant for collinear lattices, such structures suffer from low out-of-plane strength due to elastic buckling of the vertical members impeding the exploitation of more of the inherent material strength. This shortcoming is addressed in the current work by transferring the concept of stayed columns from civil engineering (e.g. see Hafez et al. 1979; Zschernack et al. 2016; Köllner et al. 2019) to collinear lattices via the design freedom provided by additive manufacturing techniques, with MEX printing being employed herein. Thus, the work aims at developing a novel type of collinear lattice structures with improved compressive strengths.

The first objective of the current work is the realisation of the additive manufacturing of stayed columns using the FFF printing method. Such stayed columns effectively represent geometric unit cells (representative elements) of collinear lattices. Following its transfer to the additive manufacturing of two-dimensional (2D) lattices, the second objective of the work is to highlight the significant improvement of the load carrying behaviour in comparison with traditional collinear lattices by means of conducting an experimental study on the compressive behaviour. Hence, additively manufactured unit cells and multi-cell/2D lattices (with and without stayed columns) are tested. The work highlights that by understanding the buckling behaviour of such unit cells, the strength of collinear lattices can be significantly improved exploiting the design freedom introduced via the additive manufacturing. Moreover, it is also shown that by deliberately introducing specific geometric imperfections in the additive manufacturing process the structural behaviour of the stayed column lattices can be manipulated.

The article is set out as follows, the concept of stayed columns is described in Sect. 2. The additive manufacturing of the unit cells and lattices is presented in Sect. 3. In Sect. 4, the experimental study is described providing information about the equipment, the implementation and the tested specimens and configurations. Results on the compressive behaviour of single unit cells and lattice structures are presented in Sect. 5, where effects of imperfections are specifically addressed. The paper closes with conclusions regarding the implementation of the concept stayed columns via additive manufacturing in collinear lattice structures.

2 Concept of stayed columns

The motivation to utilizing stayed columns to enhance the structural performance of slender collinear lattice materials under axial compression originates from the concept of pre-stressed stayed columns in civil engineering applications (see e.g. Hafez et al. (1979); Saito and Ahmer Wadee (2009); Köllner et al. (2019)). In such works, it was shown that by pre-stressing stays of columns (see Fig. 1a), the ultimate load (presumed to be effectively the buckling load) of the column can be significantly increased. In Zschernack et al. (2016) it was furthermore demonstrated that the effect of increasing ultimate/buckling load can also be achieved purely by design considerations of the stayed columns. The hindering effect of diagonal stays against buckling of the vertical member can thereby be attributed to geometric and material parameters. Figure 1b illustrates the increasing buckling loads in relationship to the effect of stays that is characterized in Zschernack et al. (2016) by a parameter K effectively representing a normalized spring stiffness depending on geometric and material parameters of the stayed-column (cf. Zschernack et al. 2016). Thus, the underlying concept appears to be ideally suited to address the inherently low compressive strength of slender collinear lattices that is governed by elastic buckling of the columns.

To highlight the effect of stays on the buckling behaviour, Fig. 2 provides an overview of possible buckling modes associated with the introduction of stays. Whereas the column without stays (Fig. 2a) remains in the first Euler mode of a column (C-mode), various responses may be triggered by introducing stays. It should be noted that increasing loads will be associated with buckling modes (b) to (c).

Buckling modes “C-mode” and “double-S-mode” illustrated in Fig. 2b and c respectively, can be associated with the zones defined by the vertical dotted line in Fig. 1b. Whenever, the hindering effect the stays is smaller than a certain threshold, then the buckling

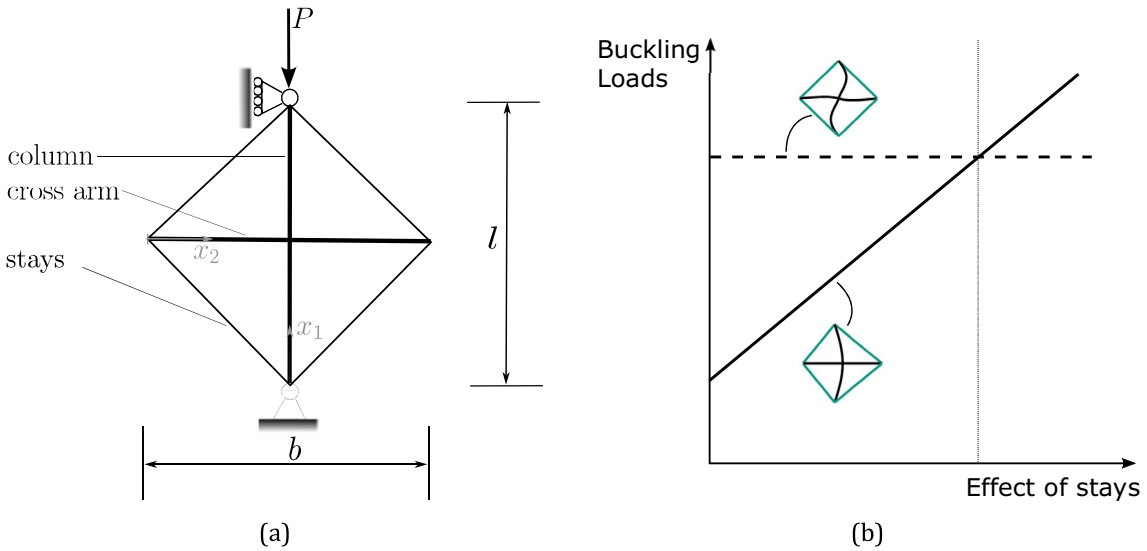

Fig. 1 Concept of stayed columns; **a** Schematic, **b** Effect of stays (geometric and material parameters) on the buckling behaviour of stayed columns

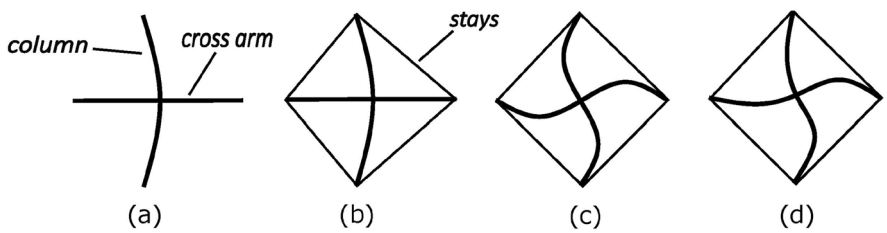

Fig. 2 Buckling modes of stayed columns; **a** No stays, **b** C-mode, **c** Double-S-mode, **d** C + double-S-mode (superposition of (**b**) and (**c**))

behaviour remains in the C-mode (associated with increasing buckling loads). For stay configurations causing an effect that is larger than the threshold, the stayed column buckles in a double-S-mode. The buckling load associated with the double-S-mode is not effected by changes in the stays, thus remains constant as visualized in Fig. 1b. When the stayed column buckles in the double-S-mode, the effect of stays is strong enough to suppress the C-mode, which is then associated with higher applied loading; effectively, the first buckling mode of the structure changes from C-mode to double-S-mode. It should be noted that the buckling load associated with the double-S-mode can be regarded as the upper limit for the buckling load of a stayed column. In Fig. 2d, a superposition of both buckling modes corresponding to an interactive buckling response is illustrated that may also be triggered for specific configurations (cf. Köllner et al. 2019) and serves to introduce imperfections within the current study (see Sects. 3 to 5).

The current study aims at exploring the concept of stayed columns within the additive manufacturing of stayed collinear lattices to develop a novel type of collinear lattice structures with improved compressive strengths. The methodology of the study is summarized in Fig. 3. Single stayed columns as well as two-dimensional (2D) assemblies of the stayed columns are additively manufactured. The single stayed column and the 2D assembly will be subsequently referred to as the (geometric) unit cell and the lattice (consisting of $m \times n$ unit cells). In an experimental study, the influence of the stays and geometric imperfections on the compressive behaviour of the unit cell (UC) and the lattice is analysed and their effect on the compressive strength is determined.

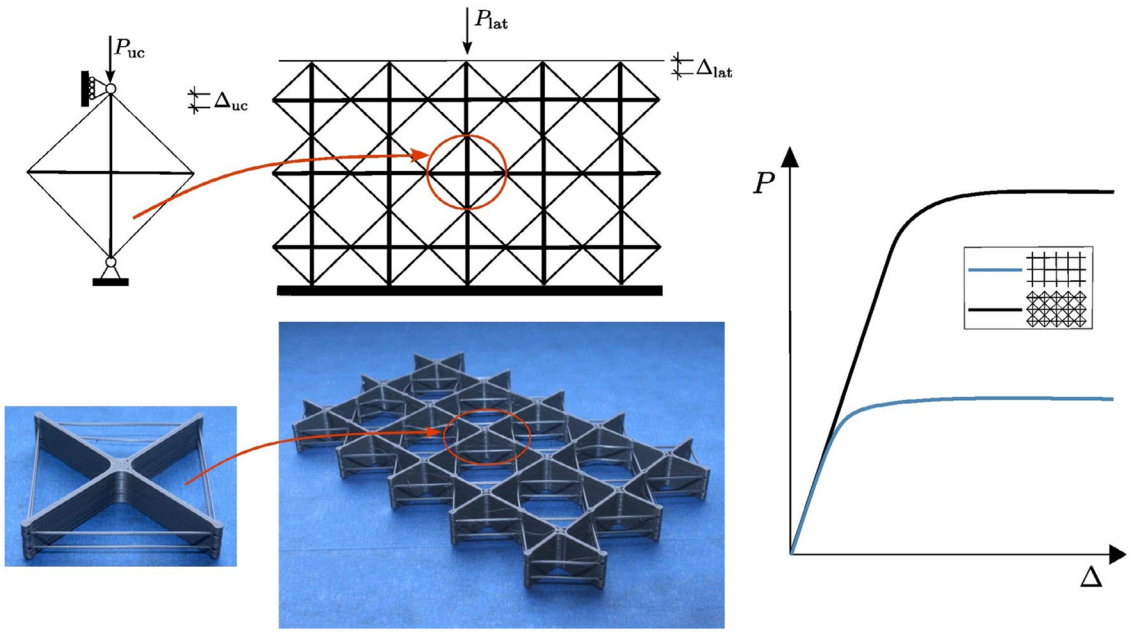

Fig. 3 Summary of the methodology of the current work

3 Additive manufacturing

In this section, the additive manufacturing is described providing information about the material extrusion additive manufacturing (MEX) printer and the materials used, the concept of bridging as well as the design and specimen production of the UCs and lattices.

3.1 Equipment

The UCs and lattices have been fabricated through additive manufacturing using the Prusa i3 MK3S+ MEX 3D printer (see a schematic in Fig. 4), developed by Prusa Research (Prusa Research a.s., Prague, Czech Republic).

The MEX 3D printing process, also known as fused filament fabrication (FFF), involves the additive manufacturing of objects by extruding a thermoplastic filament through a heated nozzle onto a build platform. The material solidifies upon deposition, enabling layer-by-layer construction of the desired three-dimensional structure. Slicer software plays a crucial role in the MEX 3D printing process. It is used to convert the digital 3D model of the desired object into a series of instructions and code called G-Code that the 3D printer can read. The slicer software "slices" the 3D model into thin horizontal layers and generates a corresponding tool path for the printer's nozzle to follow. The G-Code includes information on nozzle movement, extrusion rate, and temperature settings.

Polylactic acid (PLA) provided by Prusa Research (Prusament PLA Galaxy Silver) has been used as the printing material in this work. PLA is a biodegradable material with a tensile strength of approximately 60 MPa and an elastic modulus of approximately 3500 MPa (Farah et al. 2016). However, to obtain similar material properties as for the bulk material specific printing parameters (e.g. printing temperature, speed, flow rate, etc.) should be considered as described in Özen et al. (2021); Dönitz et al. (2023).

3.2 Specimen production

The section is subdivided into the production of the unit cells (UC) and the lattices, described in Sects. 3.2.1 and 3.2.2 respectively. The manufacturing processes employed for both specimen types, such as the bridging of the printing path, are explained in Sect. 3.2.1. The printing parameters are also provided to allow for the reproduction of the specimens.

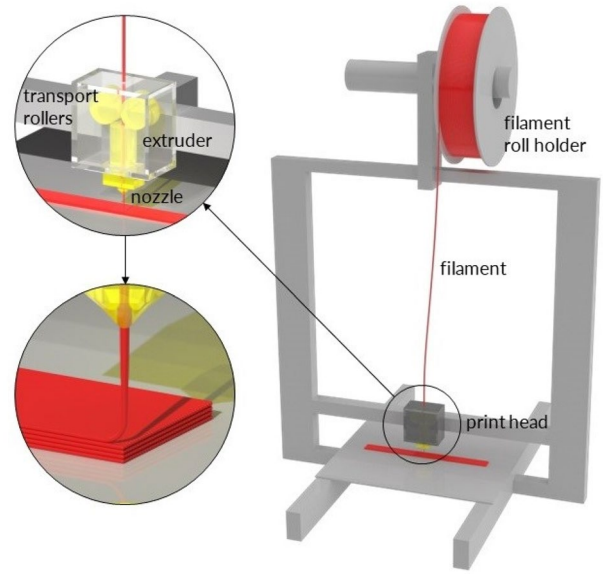

Fig. 4 Diagram illustrating the MEX 3D printing procedure following the Prusa i3MK3s specifications

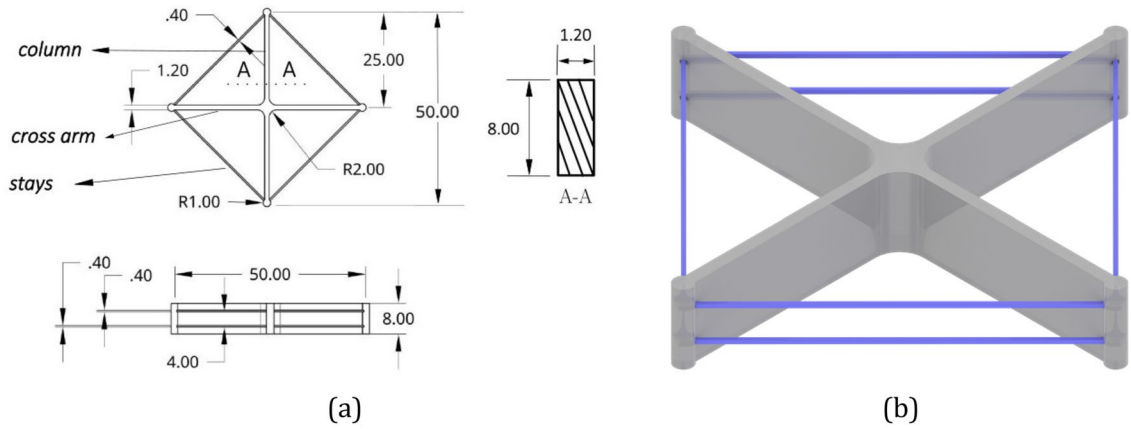

Fig. 5 **a** Technical drawing and **b** CAD model of the unit cell (UC)

3.2.1 Unit cells

The technical drawing alongside the CAD model of the UC cell is provided in Fig. 5. The UC and lattice has been modelled in Rhinoceros 3D (Rhino) (TLM, Inc. 146 N Canal St, Suite 320 Seattle, WA 98103 USA). Rhino has been selected to design the structures owing to its plugin Grasshopper, which can be used to create shapes via generative algorithms. This has been employed in the current study to implement predefined imperfections within the UCs or lattices (*cf*. Fig. 2).

A critical step in the UC design process involved ensuring that sufficient surface area is available for connecting the stays with both the column and cross arm during the printing process. To achieve this, circular endpoints have been introduced in that specific region. Beyond that, the key challenge in manufacturing the UCs and lattices is the realization of the stays that connect the endpoints of the columns. Since these stays are not directly connected to the build plate of the FFF printer or previously printed parts, a support structure would normally be required in the manufacturing. However, depending on the material

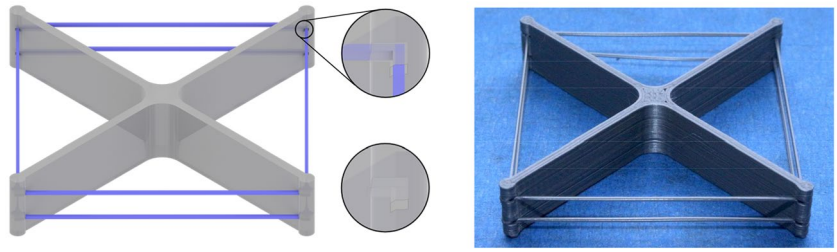

Fig. 6 Design of the UC; **a** CAD visualization of the cutout, **b** Printed UC

and the specific feature geometry, some overhanging structures can also be printed without the need for support structures which is commonly referred to as bridging. This approach has been explored in the current work to fabricate the columns without relying on support features. In preliminary tests, possible dimensions of stays (e.g. length, thickness) were determined that involved determining the specific printing methodology employed in this study. A successful implementation of the printing without support structure requires either manipulation of the G-Code of the sliced file or adjustments to the geometry. Owing to its convenience and reproducibility the latter has been employed herein. Consequently, the design of the UC was altered in the vicinity of the endpoints by introducing a cutout. This strategically positioned cutout around the stays ensures that the stays are printed separately from the rest of the columns, all in a single continuous motion. Figure 6a visualizes this design by providing a closer look at the endpoints where the cutouts with and without stays are shown. The printing of the stays (see Fig. 6b) results in a minor increase in weight by 5.1% compared to a UC without stays (1.45 and 1.38 g, respectively).

It should be stressed that further adjustments to the endpoints of the columns and cross-arms are required to ensure printing the bridge is performed seamlessly in a single continuous motion which provides the pivotal rigid connection with the underlying structure. Therefore, the cutouts are designed to be marginally wider than the stays, thus by 0.1 mm. This narrow gap effectively adjusts the printer's path without compromising the structural integrity of the unit cell. This adjustment is possible because the 3D printer's resolution is not fine enough to avoid printing the cutout, allowing for a seamless and reliable printing process that forms a rigid bond at the connections between stays and column/cross-arm.[1] The printing process highlighting the manipulated printing path through the cutouts that facilitates the print of the stays is visualized in Fig. 7.

The actual bridging printing process is shown in Fig. 8 highlighting a sequence of the additive manufacturing of the UCs, where the bridges are seamlessly printed in a single motion (cf. Fig. 7b and c).

As shown in Fig. 8, the devised method ensures that the stays are successfully printed with the bridging concept. The printing parameters used in the study are provided in Table 1.

In addition the UC specimens, UCs without stays—effectively the representative element of a collinear lattice—have also been additively manufactured. The effect of the stays on the structural response under compressive loading is highlighted by a comparative experimental study, described in Sects. 4 and 5. Moreover, the additive manufacturing of specimens with geometric imperfections has been conducted. Therefore, buckling mode shapes have been introduced in the CAD model within the software tool Rhino, which facilitates a generic implementation following pre-defined functional dependencies. Mode shapes expressed in terms of trigonometric functions (see Sect. 4) have been incorporated within the Rhino CAD model. Herein, an imperfection deemed to represent a worst-case scenario, thus a superposition of two buckling modes (cf. Fig. 2) originating from mode interactions, has been selected and additively manufactured. Figure 9

[1] Note that if the stays are linked to the columns through a basic extrusion in the design, such an optimal connection would not be achieved. This is associated with the slicing software that typically prioritizes printing the columns before the bridges, resulting in an ineffective interface between the column and stay.

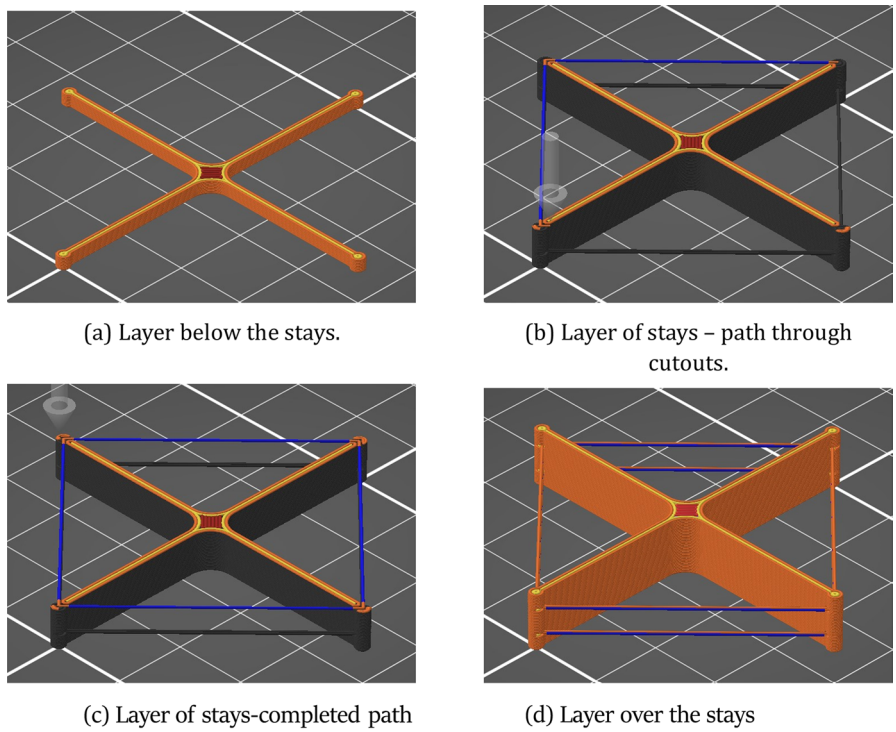

Fig. 7 Excerpts from slicing of the printing process

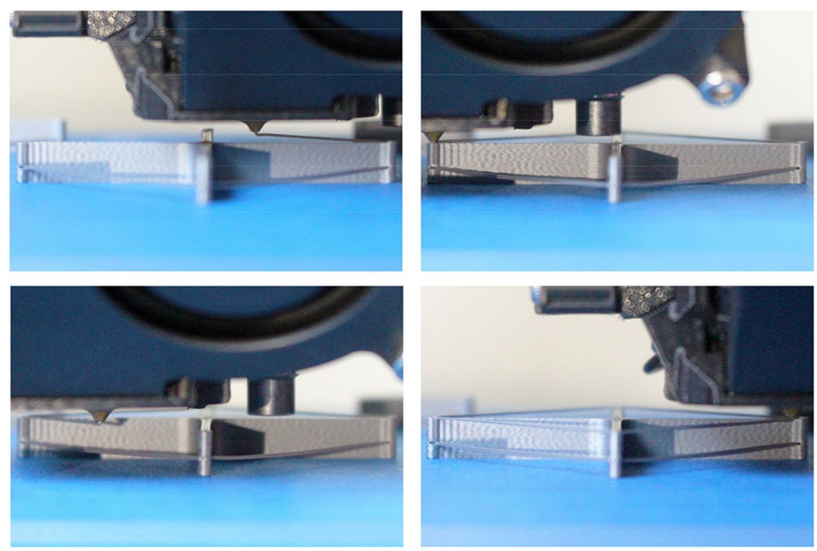

Fig. 8 Visualization of the bridging printing process

shows the CAD sketch and the printed specimen, respectively. A superposition of the C-mode and the double-S-mode has been produced (cf. Fig. 2d). The magnitude of the imperfection is expressed in terms of the amplitude of the mode shapes, where amplitudes of half and one line width, 0.2 mm and 0.4 mm respectively, have been considered. Such magnitudes are deemed to be small enough to mimic realistic manufacturing errors but also affect the structural response of the structure.

Table 1 Printing parameters as defined in PrusaSlicer

FFF 3D printer	
Printer	PRUSA i3 MK3S+
Nozzle diameter	0.4 mm
Quality	
Layer height	0.2 mm
Initial layer height	0.2 mm
Line width	0.4 mm
Walls	
Perimeters	2
TOP/BOTTOM	
Top/Bottom layers	2
Infill	
Infill density	100%
Infill pattern	Rectilinear
Material	
Printing temperature	200 °C
Build plate temperature	55.0 °C
Flow	100%
Speed	
Print speed	35.0 mm/s
Travel speed	120.0 mm/s
z Hop speed	12.0 mm/s
First layer speed	60%
Travel	
Enable retraction	on
Retraction distance	0.8 mm
Retraction speed	35.0 mm/s
Avoid printed parts when traveling	On
Z Hop when retracted	On
Z Hop height	1.0 mm
Cooling	
Fan speed	100%
Disable fan for first	1 layers

3.2.2 Lattices

To demonstrate the effect of stays on a collinear lattice structure, 2D lattices assembled of the UCs (cf. Sect. 3.2.1) have been additively manufactured. The technical drawing of the lattice is provided in Fig. 10. In the additive manufacturing, the same printing method for manufacturing the stays with bridging as described in Sect. 3.2.1 has been employed.

A 5×3 lattice configuration, thus five UCs in horizontal and three UCs in vertical direction, has been chosen for this study. This ensures that the lattices comprise UCs at the supports, at the free edge and within the lattice. Therefore, the dimensions of the UCs have been reduced. The additive manufacturing of the UCs requires a width of the columns and cross-arms of at least two line width, thus 0.8 mm (cf. Table 1), where the length and width of the UCs have been selected to ensure that elastic buckling remains the initial failure mode of the structure as well as to comply with the dimensions of the supports available for the testing machine. The incorporation of the stays within the lattice results in a minor increase in weight by 7.6% compared to a lattice without stays (5.41 g and 5.03 g, respectively).

In addition to the additive manufacturing of perfect lattices, imperfect lattice where a specific mode shape has been assigned to a UC in the middle of the lattice as highlighted in red Fig. 10. The choice and purpose of this imperfection is described in Sect. 4. In Fig. 11, the CAD model and the printed specimen are shown. The lattices have been printed with the same set of parameters as for the UCs (see Table 1) that have been found to ensure reliable prints of good quality which enables to manufacture the stays by bridging.

4 Experimental test programme

The experimental study comprises two test series: (i) Uniaxial compression tests of the UCs, and (ii) Uniaxial compression tests of the lattices. All tests have been conducted on the testing machine ZwickRoell Z2.5 (ZwickRoell GmbH & Co. KG August-Nagel-Straße 11, 89079 Ulm, Germany) with a nominal maximum load of 2.5 kN. The experimental test programme for the UCs and the lattices is described next in Sects. 4.1 and 4.2, respectively. The results of the experimental tests are provided and discussed in Sects. 5.1 and 5.2.

4.1 Uniaxial compression tests of unit cells

Compression tests of perfect UCs and UCs with an imperfection have been conducted. For the imperfect cells, an imperfection shape in the form of a superposition of the C and double-S-modes (see Sect. 2) are chosen, deemed to represent a buckling response of the worst-case scenario of mode interactions (cf. Zschernack et al. 2016). An overview of the configurations is provided in Table 2.

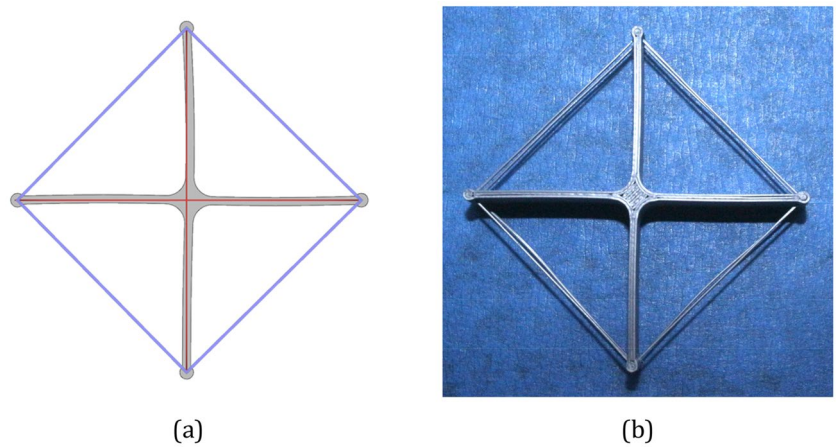

Fig. 9 UCs with a C- and double-S-mode imperfection; **a** CAD sketch, **b** printed specimens

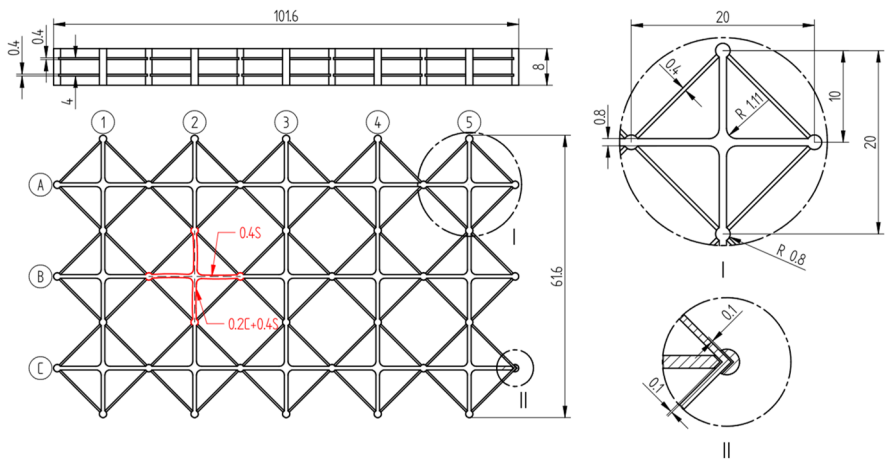

Fig. 10 Technical drawing of the additively manufactured lattice

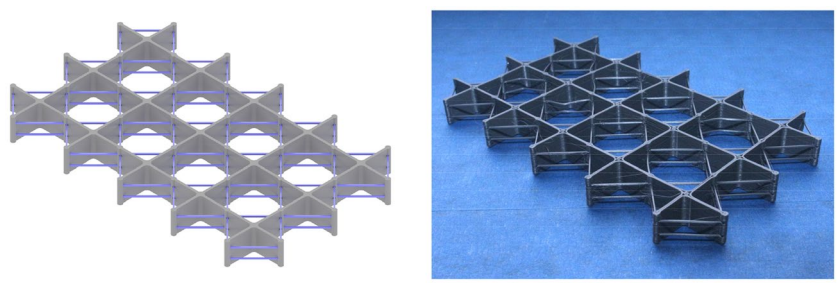

Fig. 11 Design of the lattice; **a** CAD model, **b** printed lattice

The imperfection described in Table 2 correspond to the following shape of the column and cross-arm (cf. Fig. 2), thus: C-mode—the column has a lateral deflection in the form of $A\sin\left(\pi x_1/l\right)$ (note: there is no deflection in the cross-arm); double-S-mode—the column and the cross-arm have the shapes $B\sin\left(2\pi x_1/l\right)$ and $B\sin\left(2\pi x_2/l\right)$, with A and B being 0.2 mm and 0.4 mm, respectively, for the tested imperfect cell.

The UC tests have been conducted under applied end-shortening with a test speed of 0.2 mm/min that enables to capture the (non)linear buckling response of the structures. The analysis has been limited up to a deformation state where a clear post-buckling

Table 2 Overview of tested UC configurations

#	Label	Tests	Description
1	UC_1	8	UC without stays
2	UC_2	8	Perfect UC with stays
3	UC_3	8	C-mode and double-S-mode imperfections; 0.2 C+0.4 S, 0.2 mm amplitude (C-mode), 0.4 mm amplitude (double-S-mode)

response is established and failure is predominantly associated with plastic deformation (ca. 1 mm of applied end-shortening). A simply supported test setup has been facilitated by additively manufacturing supports with a U-shape half-cylinder-like notch with a radius slightly larger than the end-points of the specimens. This enables the correct alignment of the specimens and the 'free' rotation at the end-points as required in simply supported systems. However, effects resulting from friction should be considered within the evaluation of the experiments. It should be noted that, in the post-processing of the experimental test data (UCs and lattices), the initial nonlinear response, as characteristic for compression tests (see ASTM D695–15. 2019) and associated with the effects of initial settling and aligning of the specimens and supports, is extracted from the data following the method proposed in ASTM D695–15. (2019). Therefore, the slope of the 'effectively linear' response is determined and taken as the initial structural response, thus shifting the slope onto the origin of the load–displacement graph. This post-processing step alongside the statistical analysis and the illustration of the experimental results has been performed with a python script.

Per configuration eight specimens have been tested to enable a statistical analysis of the results in terms of determining mean curves of the load–displacement response with the 95% confidence interval as well as the means of the ultimate load. In addition, single tests are evaluated in Sect. 5.1 to highlight characteristic mechanical behaviours observed in the experiments. In the experiments, in addition to the load and displacement information from the testing machine, videos and images have been recorded during the tests to visualize the deformation behaviour. Note that files to reproduce the additive manufacturing of the specimens (UCs and lattices) are provided as supplementary data.

Table 3 Overview of tested lattices configurations

#	Label	Tests	Description
1	Lat_1	8	Lattice without stays
2	Lat_2	8	Perfect lattice with stays
3	Lat_3	8	Imperfect lattice with stays, imperfection in cell B2

4.2 Uniaxial compression tests of the lattices

As done for the UC specimens, tests with perfect and imperfect lattices have been conducted. The dimensions and the assembly of the lattices is provided in Fig. 10. Three configurations have been studied in the experimental tests, which are outlined in Table 3. With the configurations tested, the effect of adding stays to collinear lattices will be highlighted alongside evaluating the influence of introducing deliberately specified imperfections within such lattices.

The imperfection in "Lat_3"has been assigned to a cell which is not adjacent to the supports nor the free edges. The intention has been to study whether and how failure in form of elastic buckling propagates through the lattice. Thus, the worst-case imperfection as considered in the UC tests (see Sects. 4.1 and 5.1), i.e. configuration 0.2 C + 0.4 double-S-mode, has been assigned to cell B2 (see Fig. 10) during the additive manufacturing of the lattices.

The test have been conducted with a speed of 0.5 mm/min deemed to provide a sufficiently slow loading to trace the failure behaviour of the lattices which has been established in preliminary tests. Owing to the simplified alignment of the specimen in comparison with the UCs, flat aluminium supports have been used in this study. As done for the UC tests, eight specimens have been tested for each

configuration in Table 3 to enable a statistical analysis of the results. The results comprise mean curves of the load–displacement response with the 95% confidence interval and the means of the ultimate load. Single tests are also evaluated in Sect. 5.2 to highlight characteristic mechanical behaviours. Videos and images have also been recorded during the tests to visualize deformation characteristics.

5 Results

Results for compression tests of UCs and lattices are presented in Sects. 5.1 and 5.2 respectively. The compressive behaviour is studied by evaluating the load against end-shortening response where mean curves and single tests alongside footage of deformation characteristics are analysed.

5.1 Unit cell

In Fig. 12, the results of the comparative study between unit cells of collinear lattices with and without stays is provided in the form of mean curves of the load vs. end-shortening behaviour exhibiting the 95% confidence interval (Fig. 12a) and the load–displacement responses of single tests where characteristic deformation shapes from the experiments are provided (Fig. 12b).

In addition to providing quantitative information on load and end-shortening, Fig. 12a also visualizes the factor of load increase between the UC with stays (black line) and without stays (blue line) by an additional ordinate on the right hand side of Fig. 12a. The "load increase factor" relates the ultimate load (P_{ult} in Fig. 12a) to the buckling load of the UC without stays ("UC_1") which is experimentally determined in Fig. 12a by determining the intersection point of the tangents of the fundamental path (evaluated at the origin) and the post-buckling paths (evaluated at the plateau of the post-buckling response illustrated by the blue line). For the UCs with and without stays, the confidence interval is provided by a shaded black and blue area, respectively.

The effect of the stays on the load carrying capacity of the UCs is clearly demonstrated in Fig. 5a. Initially, both types of UCs show a similar load–displacement response. However, with the stays preventing the column to buckle, loads significantly higher than the ultimate load of the UC without stays (blue line) are attained by the UC with stays (black line). Until the UC reaches its buckling load, the column and cross-arm remain straight. At a load increase factor of approx. 4.46, the ultimate load of the UC is reached that corresponds to the buckling load of the structure. It should be stressed that such significant increase in load is achieved by adding just 5.1% in weight to the UC (see Sect. 3.2.1). Thus, the specific compressive strength of the UC, i.e. the strength per weight of the specimens, increases by 324% through adding the stays during the additive manufacturing. The post-buckling response is characterized by slightly decreasing loads indicating a structurally unstable post-buckling behaviour (under load control). It should be noted that the pre- and post-buckling response exhibits a very small 95% confidence interval that underlines the repeatability of the results, where a slightly larger interval is present around the ultimate load.

Figure 12b visualizes the buckling behaviour of the UCs by relating buckling shapes with single characteristic experimental tests. The increase in load carrying capacity of the UCs with stays is associated with the buckling mode changing from the C-mode for the UC without stays (see footage corresponding to the blue line in Fig. 12b) to a double-S-mode shape for UC with stays (see footage corresponding to the black line). By introducing the stays to the UCs, as explained in Sect. 2, the double-S-mode shape becomes the first buckling mode of the structure, whereas the C-mode shifts to larger load levels.

The effect of imperfections on the structural behaviour is visualized in Fig. 13 by adding the mean load vs. end-shortening curve for the imperfect cell (red line and shaded area). Owing to the initial non-axial displacement, the imperfection reduces the compressive stiffness of the UC in comparison with the perfect configurations. Moreover, the ultimate load reduces significantly in comparison with the perfect UC with stays (black line). In contrast, the imperfection resolves the limit/peak load behaviour as observed for perfect structures, where increasing loading has been obtained throughout the range investigated in Fig. 13a. It should be noted that the buckling shapes corresponding to distinct applied load levels (indicated by dark red dots in Fig. 13a), provided in Fig. 13b to d, highlight an amplification of the double-S-mode with vanishing C-mode contributions.

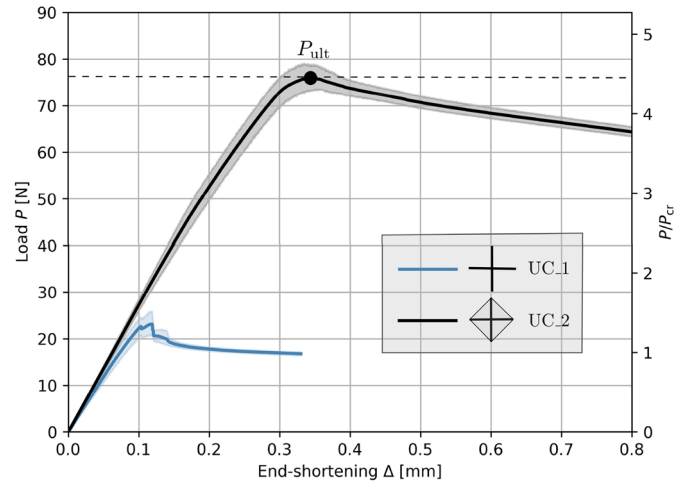

(a) Load vs. end-shortening for UC 1 and UC 2; mean curves; normalized load provided on the ordinate on th right hand side.

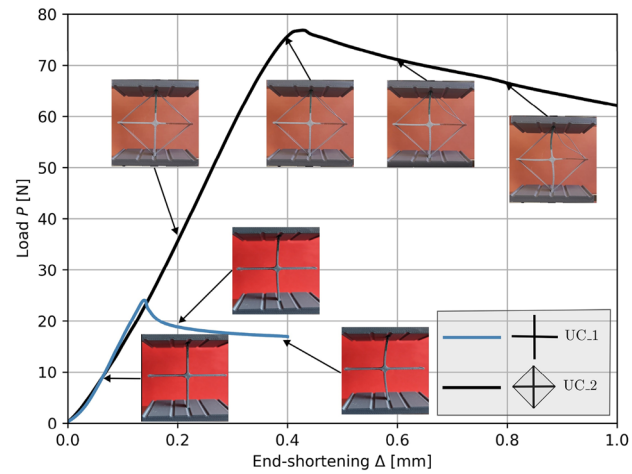

(b) Load vs. end-shortening for UC 1 and UC 2; single tests with images of characteristic buckling deformation.

Fig. 12 Experimental results for the UC tests; perfect UCs without (UC_1) and with stays (UC_2); load vs. end-shortening behaviour; **a** mean curves; **b** single characteristic tests with associated (buckling) deformation

As a consequence, the imperfect curve will slowly converge onto the perfect curve that exhibits the same post-buckling mode shape. This is highlighted in Fig. 13a by the imperfect and perfect curves almost having the same load levels at the end of the applied end-shortening considered in this study.

5.2 Lattice

The results of the comparative study between collinear lattices with and without stays are provided in Fig. 14. The mean curves of the load vs. end-shortening behaviour exhibiting the 95% confidence interval and the load–displacement responses of single tests where characteristic deformation shapes from the experiments are provided in Fig. 14a and b, respectively. As for the UCs, the responses for the lattices with the stays and without stays are visualized in black and blue, respectively.

Evaluating the increase in ultimate load (P_{ult}) associated with introducing the stays during the additive manufacturing of the lattices, a similar factor as for the UCs can be determined with ca. 4.40. Slightly more weight is added to the structure (ca. 7.6%) through the addition of stays in comparison with the UCs. This relates to the smaller lengths of the columns and cross-arms used in the study on

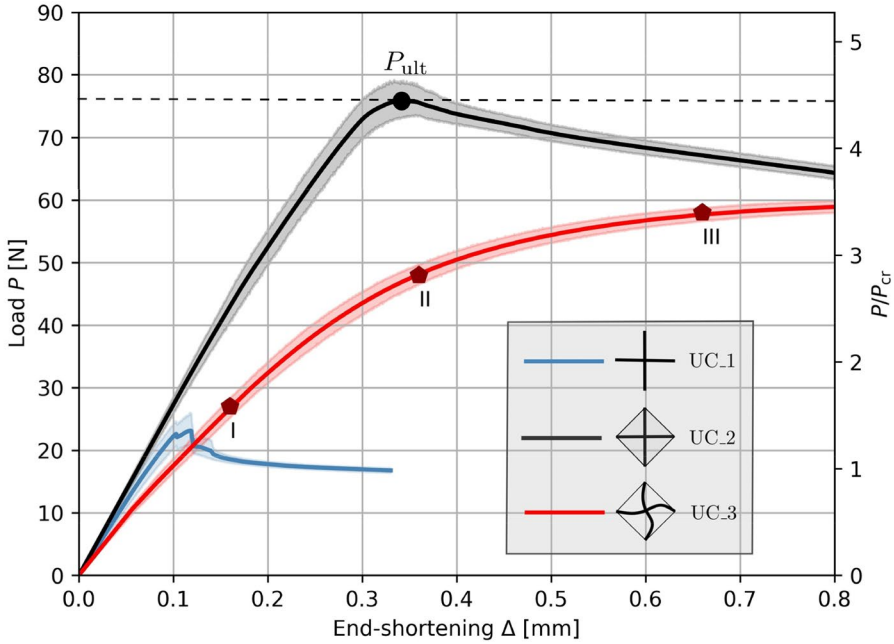

(a) Load vs. end-shortening for UC 1, UC 2 and UC 3; mean curves; normalized load provided on the right hand side ordinate.

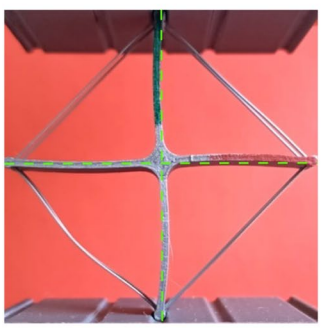

(b) Buckling deformation at (I).

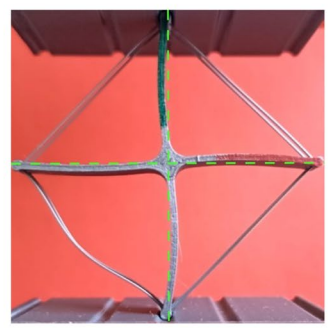

(c) Buckling deformation at (II).

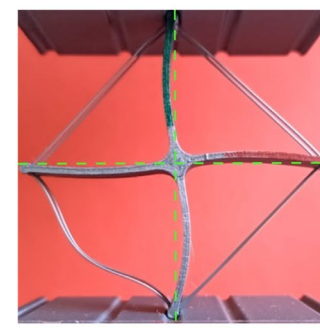

(d) Buckling deformation at (III).

Fig. 13 Effect of imperfections on the compressive behaviour of UCs; **a** Load vs. end-shortening behaviour, (**b–d**) characteristic buckling deformation of UC_3 (UC with stays and imperfection; dashed green line indicates the undeformed shape of a perfect UC)

lattices. The specific compressive strength increases by ca. 309% comparing lattice with and without stays.

In terms of the buckling behaviour, the lattice without stays shows a characteristic weakly stable initial buckling response corresponding to the plateau in loading between end-shortenings of 0.5 mm and 1.5 mm, shown Fig. 14a and b. The decreasing loads for larger applied end-shortenings are associated with the onset of inelastic deformations that is also documented by the localizations in the buckling mode shapes provided in Fig. 14b for the blue line. The buckling mode shape is a C-mode spreading over the entire height of the lattice, which will be referred to as a global C-mode. The lattice with stays (black line in Fig. 14b) exhibits a sharp drop in load after the ultimate load of the structure is reached. Around the ultimate load, the buckling remains locally within certain UCs showing minor double-S-mode responses (see first footage of the buckling mode for the black line in Fig. 14b).The sudden drop in load corresponds to the buckling response jumping out of a local displacement within

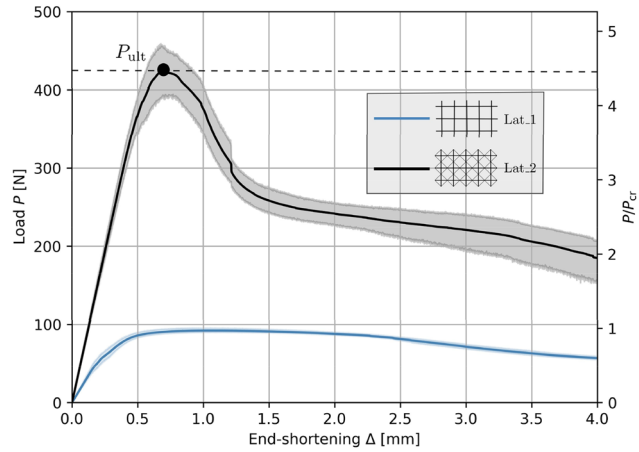

(a) Load vs. end-shortening for Lat 1 and Lat 2; mean curves; normalized load provided on the right hand side ordinate.

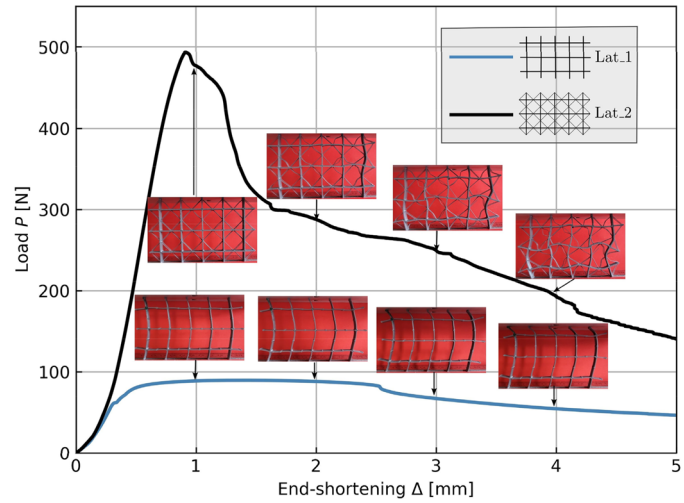

(b) Load vs. end-shortening for Lat 1 and Lat 2; single tests with images of characteristic buckling deformation.

Fig. 14 Experimental results for the lattice tests; perfect lattice without (Lat_1) and with stays (Lat_2); load vs. end-shortening behaviour; **a** mean curves; **b** sSingle characteristic tests with associated (buckling) deformation

the UCs to global modes indicating a global S-mode response, visualized in the second and third footage of the buckling mode for the black line in Fig. 14b. Ultimately, if not impeded by significant inelastic deformation, the buckling mode jumps to a global C-mode, as observed for the lattice without stays. It should be noted that such jumps in mode shapes are partly associated with stays rupturing and thus releasing the local buckling response of the UCs.

As for the UCs, the effect of imperfections on the structural behaviour of the lattices is visualized in Fig. 15 by adding the mean load vs. end-shortening curve for the imperfect lattice (red line and shaded area). Some of the effects observed for the UCs can also be obtained for the lattices having a local imperfection assigned to a single UC. Thus, the compressive stiffness of the imperfect lattice is lower than for the perfect configurations. The ultimate load is also reduced. On the other hand, the imperfection lowers the severity of the drop in load after reaching the ultimate load. However, in contrast to the UCs, the same qualitative behaviour after reaching the ultimate load can be observed comparing perfect and imperfect lattices. This is highlighted in Fig. 15a, where red and black lines are almost coinciding in the post-buckling range. It should be noted that by introducing the imperfection to cell B2 (cf. Fig. 10), the buckling behaviour observed for the

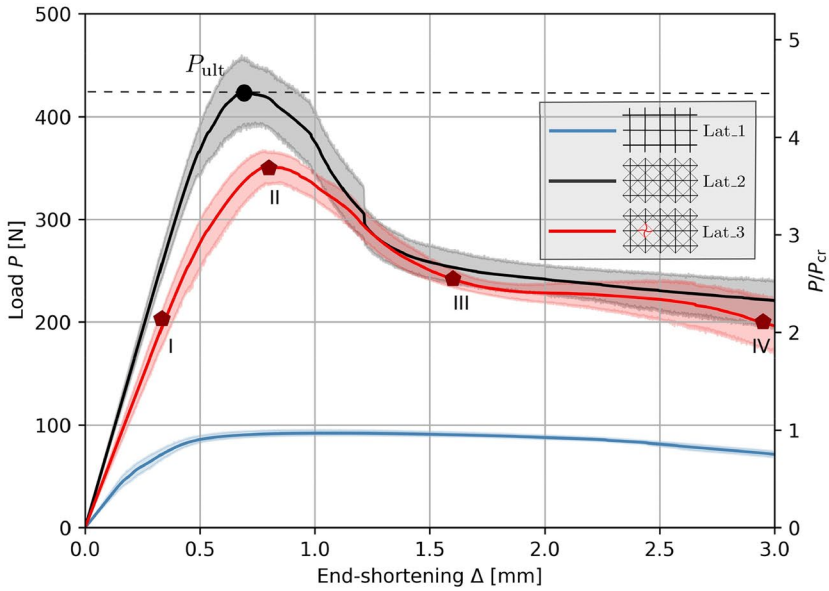

(a) Load vs. end-shortening for Lat 1, Lat 2 and Lat 3;
mean curves; normalized load provided on the right hand side ordinate.

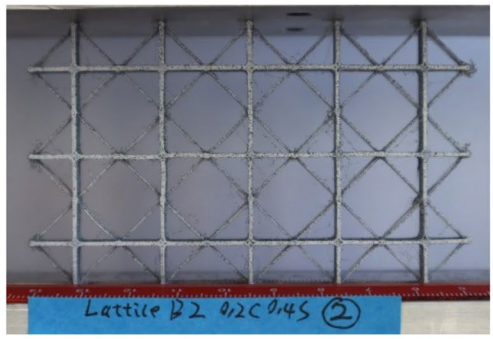

(b) Deformation at (I)

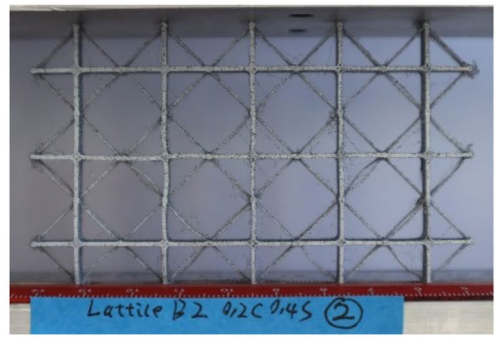

(c) Deformation at (II)

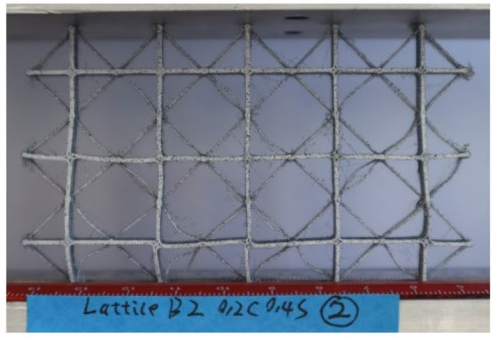

(d) Deformation at (III)

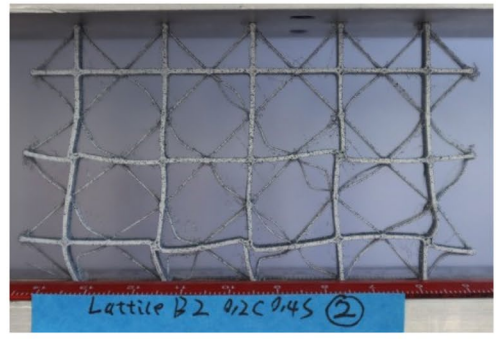

(e) Deformation at (IV)

Fig. 15 Effect of imperfections on the compressive behaviour of lattices; **a** Load vs. end-shortening behaviour, (**b**–**d**) characteristic buckling deformation of Lat_3 (lattice with stays and imperfection)

Table 4 Summary of the results on the increasing load-carrying capacities of UCs and lattices

	Load increase factor	Increase in specific strength (%)
UCs	4.46	324
Lattices	4.40	309

perfect lattice, occurs less abruptly so that Fig. 15b to d underline the transition from a local double-S-mode shape to global S-modes that localizes deep in the post-buckling range (see Fig. 15e). Due to the imperfection, the mode jumping is less pronounced than for the perfect lattice. The result shows that the structural response can be manipulated deliberately by introducing such imperfections.

The increases in out-of-plane compressive strength for the UCs and lattices are summarized in Table 4. The results highlight that the improvement of the out-of-plane compressive strength can be transferred from the UC level to 2D lattices. The significant increase in ultimate loading, highlighted by the load increase factor in Table 4, is slightly lowered by evaluating the quantity specific compressive strength (strength per weight) that takes into consideration the minor additional material that must be used for printing the stays (see Sects. 3.2.1 and 3.2.2). However, increases of specific strength of 324 and 309% for UCs and lattices respectively, underline the significant effect that implementing such stays has on the structural performance of collinear lattices.

6 Conclusions

The current study has successfully demonstrated that the (specific) compressive strength of collinear lattices can be significantly improved by introducing the concept of stayed columns through additive manufacturing technologies. While requiring just minor increases in weight for printing the stays, the load carrying capacity of collinear lattices could be more than quadrupled; a load increase factor of ca. 4.40 has been determined that corresponds to an increase in specific compressive strength of 309%. It has been demonstrated that this effect can be transitioned from a single unit cell to 2D lattices. Thus, the work highlights a most promising strategy to reduce one of the major drawbacks of collinear lattices, thus the low out-of-plane compressive strength due to their vulnerability to elastic buckling.

The additive manufacturing of stayed unit cells and lattices has been achieved by employing the concept of bridging, thus: the stays are printed "on air" to connect columns and cross-arms. With specific modifications to the CAD model of columns and cross-arms, i.e. the introduction of cut-outs, the printing path of the additive manufacturing could be successfully manipulated to enable a reliable printing of such bridges. This printing strategy is pivotal for a successful production of additively manufactured stayed lattices.

By introducing imperfections in the additive manufacturing through implementing buckling mode shapes with the CAD software tool Rhino, the structural response of lattices can be altered, where failure may be initiated at predetermined unit cells of lattices. The work has highlighted that this effect should be explored in more detail in future studies. It should be noted that the addition of stays to collinear lattices extends the optimization potential of such structures regarding load carrying capacity and predetermined structural responses. Therefore, the influence of the stay geometry, material parameters as well as dimensions of the unit cells should be explored for which the current work provides the initial step.

Acknowledgements The authors want to thank Mr. Arion Juritza (TU Berlin) for his support in conducting the experimental test study. The exploration of the bridging concept in preliminary work by Mr. Ando Jacobi and Mr. Jan Holldorb is also acknowledged by the authors.

Funding Open Access funding enabled and organized by Projekt DEAL.

Data availability Data for the additive manufacturing of the UCs and lattices presented in this work are provided on GitHub at https://github.com/SVFS-TUBerlin/AM_Lattice. Raw data from the experiments can be provided upon request from the corresponding author.

Declarations

Conflict of interest The authors declare that there is no conflict of interest.

References

ASTM D695–15.: Standard test method for compressive properties of rigid plastics. West Conshohocken, PA, USA (2019)

Aamer, N., Ozkan, G., Billah Kazi, M., Masum, E.O., Jingchao, J., Jiayu, S., Sajjad, Hussain: Multi-material additive manufacturing: a systematic review of design, properties, applications, challenges, and 3D printing of materials and cellular metamaterials. Mater. Design **226**, 111661 (2023). https://doi.org/10.1016/j.matdes.2023.111661

Acanfora, V., Sellitto, A., Russo, A., Zarrelli, M., Riccio, A.: Experimental investigation on 3D printed lightweight sandwich structures for energy absorption aerospace applications. Aerosp. Sci. Technol. **137**, 108276 (2023). https://doi.org/10.1016/j.ast.2023.108276

Antonia, D., Anton, K., Tim, R., Oliver, L., Dietmar, A., Christina, V.: Additive manufacturing of biodegradable hemp-reinforced polybutylene succinate (PBS) and its mechanical characterization. Polymers **15**(10), 2271 (2023). https://doi.org/10.3390/polym15102271

Arda, Özen., Emek, Abali Bilen, Christina, Völlmecke., Jonathan, Gerstel, Dietmar, Auhl: Exploring the role of manufacturing parameters on microstructure and mechanical properties in fused deposition Modeling (FDM) using PETG. Appl. Compos. Mater. **28**(6), 1799–1828 (2021). https://doi.org/10.1007/s10443-021-09940-9

Askari, M., Hutchins, D.A., Thomas, P.J., Astolfi, L., Watson, R.L., Abdi, M., Ricci, M., et al.: Additive manufacturing of metamaterials: a review. Addit. Manufact. **36**, 101562 (2020). https://doi.org/10.1016/j.addma.2020.101562

Braga Daniel, F.O., Tavares, S.M.O., Da Silva Lucas, F.M., Moreira, P.M.G.P., De Castro Paulo, M.S.T.: Advanced design for lightweight structures: review and prospects. Prog. Aerosp. Sci. **69**, 29–39 (2014). https://doi.org/10.1016/j.paerosci.2014.03.003

Can, T., Junwei, L., Yang, Y., Ye, L., Shiping, J., Wenfeng, H.: Effect of process parameters on mechanical properties of 3D printed PLA lattice structures. Compos. Part C Open Access **3**, 100076 (2020). https://doi.org/10.1016/j.jcomc.2020.100076

Frank, C.: Current trends in automotive lightweighting strategies and materials. Materials **14**(21), 6631 (2021). https://doi.org/10.3390/ma14216631

Gorguluarslan, R.M., Gandhi, U.N., Song, Y., Choi, S.-K.: An improved lattice structure design optimization framework considering additive manufacturing constraints. Rapid Prototyp. J. **23**(2), 305–319 (2017). https://doi.org/10.1108/RPJ-10-2015-0139

Hafez, H.H., Temple, M.C., Ellis, J.S.: Pretensioning of single-crossarm stayed columns. J. Struct. Div. ASCE **105**(ST2), 359–375 (1979). https://doi.org/10.1061/JSDEAG.0005098

Köllner, A., Todt, M., Ganzosch, G., Völlmecke, C.: Experimental and numerical investigation on pre-stressed lattice structures. Thin-Walled Struct. **145**, 106396 (2019). https://doi.org/10.1016/j.tws.2019.106396

Li, M., Song, Y., Yang, X., Zhang, K.: Lattice structure design optimization under localized linear buckling constraints. Comput. Struct. **286**, 107112 (2023). https://doi.org/10.1016/j.compstruc.2023.107112

Njuguna, J.: Lightweight composite structures in transport: design manufacturing, analysis and performance. Woodhead publishing, UK (2016)

Saito, D., Ahmer Wadee, M.: Buckling behaviour of pre-stressed steel stayed columns with imperfections and stress limitation. Eng. Struct. **31**(1), 1–15 (2009). https://doi.org/10.1016/j.engstruct.2008.07.006

Shady, F., Anderson Daniel, G., Robert, L.: Physical and mechanical properties of PLA, and their functions in widespread applications—A comprehensive review. Adv. Drug Deliv. Rev. **107**, 367–392 (2016). https://doi.org/10.1016/j.addr.2016.06.012

Tobias, M., Martin, L., Bill, L., Xuezhe, Z., Ma, Q., Omar, F., Milan, Brandt: SLM lattice structures: properties, performance, applications and challenges. Mater. Design **183**, 108137 (2019). https://doi.org/10.1016/j.matdes.2019.108137

Wang, Y., Li, S., Ying, Yu., Xin, Y., Zhang, X., Zhang, Q., Wang, S.: Lattice structure design optimization coupling anisotropy and constraints of additive manufacturing. Mater. Design **196**, 109089 (2020). https://doi.org/10.1016/j.matdes.2020.109089

Zschernack, C., Ahmer Wadee, M., Völlmecke, C.: Nonlinear buckling of fibre-reinforced unit cells of lattice materials. Compos. Struct. **136**, 217–228 (2016). https://doi.org/10.1016/j.compstruct.2015.09.059